Supporting Information for

"Highly Efficient Photo/Electrocatalytic Reduction of Nitrogen into Ammonia by Dual-metal Sites"

Shiyan Wang, Li Shi, Xiaowan Bai, Qiang Li, Chongyi Ling and Jinlan Wang*

School of Physics, Southeast University, Nanjing 211189, China

*E-mail: jlwang@seu.edu.cn.

Table S1. Computed formation energy (E_f) and dissolution potential (U_{diss}) of dual-metals, U^o_{diss} and N_e are the standard dissolution potential of bulk metal and the number of transferred electrons involved in the dissolution, respectively. The electrochemically unstable systems are depicted by **red** color. $N_e = [N_e(TM1)+N_e(TM2)]/2$, $U^o_{diss} = [U^o_{diss}(TM1) + U^o_{diss}(TM2)]/2$.

Metal	N_e	U^o_{diss}(V)	E_f(eV)	U_{diss}(V)
TiCr	2	-1.27	-3.95	0.71
TiMn	2	-1.41	-4.34	0.76
TiFe	2	-1.04	0.86	-1.47
TiCo	2	-0.96	-1.75	-0.08
TiNi	2	-0.95	-1.17	-0.36
TiMo	2.5	-0.88	-2.91	0.28
TiW	2.5	-0.78	-1.97	0.01
CrMn	2	-1.05	-4.64	1.27
CrFe	2	-0.68	-3.52	1.08
CrCo	2	-0.60	-2.99	0.90
CrNi	2	-0.59	1.26	-1.22
CrMo	2.5	-0.52	0.83	-0.94
CrW	2.5	-0.42	-5.71	1.86
MnFe	2	-0.82	-3.97	1.17
MnCo	2	-0.74	-3.44	0.99
MnNi	2	-0.73	-1.59	0.07
MnMo	2.5	-0.66	-3.90	0.90
MnW	2.5	-0.56	-2.92	0.61
FeCo	2	-0.37	-2.10	0.69
FeNi	2	-0.36	-1.42	0.36
FeMo	2.5	-0.29	-2.34	0.65

FeW	2.5	-0.19	2.00	-0.99
CoNi	2	-0.27	-0.77	0.12
CoMo	2.5	-0.21	1.80	-0.93
CoW	2.5	-0.11	1.49	-0.71
NiMo	2.5	-0.19	-0.78	0.52
NiW	2.5	-0.10	0.51	-0.30
MoW	3	-0.03	-1.78	0.56

Table S2. Q_1 and Q_2 represent charge transfer from dual-metals sites to N_2 and N_2H, respectively. Q_3 [Q_2(Mo)-Q_2(Fe, Ti, Ni or W)] represent charge transfer from TM1 to TM2. Q_1 and Q_2 are relative to the charge of M1M2/g-C_3N_4.

Metal	Q_1		Q_2		Q_3
MoMo	Mo1	Mo2	Mo1	Mo2	~0.00
	0.24	0.27	0.54	0.53	
FeMo	Fe	Mo	Fe	Mo	0.43
	0.11	0.24	0.09	0.52	
TiMo	Ti	Mo	Ti	Mo	0.33
	0.19	0.28	0.21	0.54	
NiMo	Ni	Mo	Ni	Mo	0.36
	0.15	0.26	0.16	0.52	
MoW	W	Mo	W	Mo	0.38
	0.14	0.25	0.15	0.53	

Table S3. Calculated ΔZPE and TΔS of gas molecules and intermediates on catalyst, the * represent end-on mode, while ** represent side-on mode.

species	ΔZPE (eV)	TΔS (eV)	Species	ΔZPE (eV)	TΔS (eV)
N_2	0.14	0.59	NH_3	0.85	0.60
H_2	0.27	0.40	H*	0.17	0
N≡N**	0.22	0.10	N≡N*	0.23	0.11
N=NH**	0.46	0.11	N=NH*	0.53	0.15
NH−NH**	0.80	0.18	NH−NH*	0.88	0.12
NH−NH_2**	1.14	0.11	NH−NH_2*	1.21	0.15
NH_2−NH_2**	1.47	0.15	NH_2−NH_2*	1.52	0.20
NH_2−NH_3**	1.70	0.13	NH*	0.33	0.06
NH_2**	0.66	0.14	N*	0.08	0.06
NH_3**	0.98	0.16	N−NH_2*	0.81	0.14

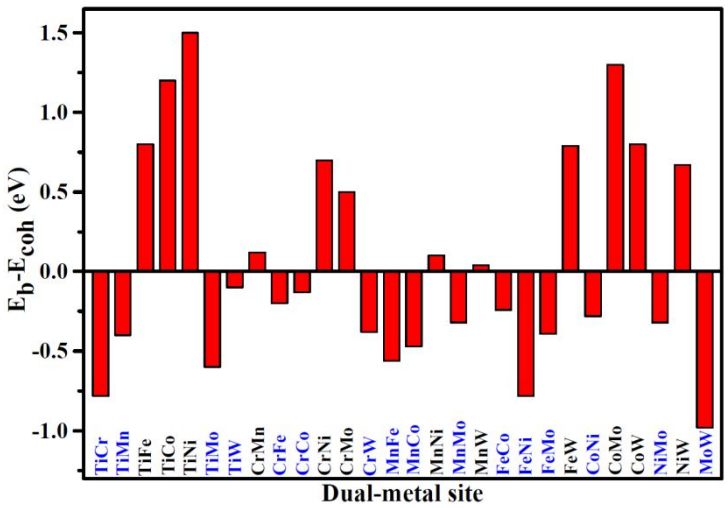

Figure S1. Energy difference between the adsorption energy (E_b) of metal dimers anchored on g-C_3N_4 and the cohesive energy (E_{coh}) of metal atoms in their crystals.

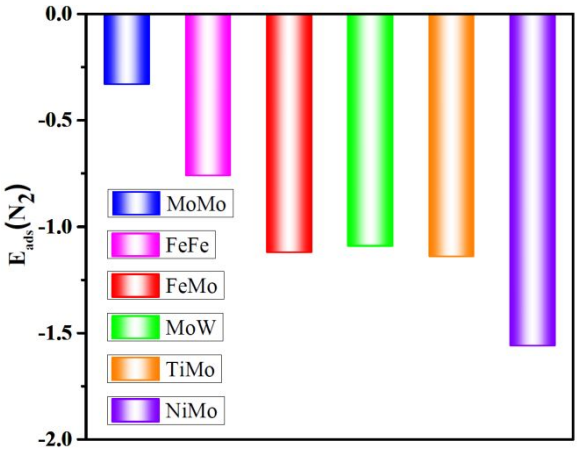

Figure S2. Adsorption energy of N_2 on MoMo, FeFe, FeMo, MoW, NiMo and TiMo dimers.

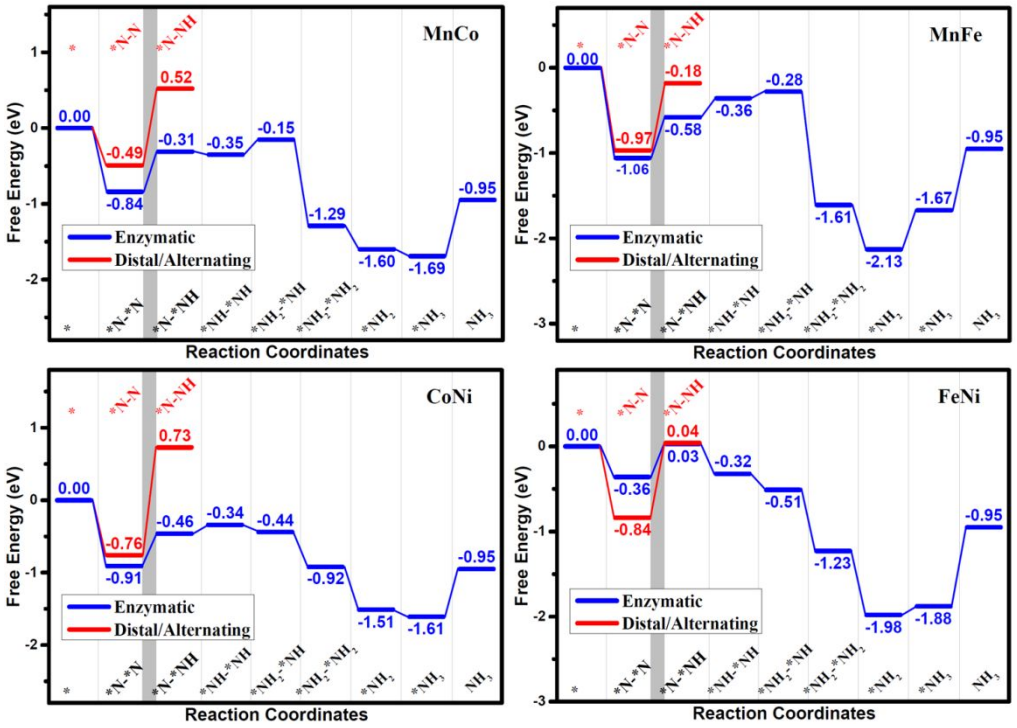

Figure S3. Free energy diagrams for NRR at zero potential on MnCo/g-C_3N_4, MnFe/g-C_3N_4, CoNi/g-C_3N_4, FeNi/g-C_3N_4 along distal, alternating and enzymatic mechanisms. The protonation process of $*N_2 + (H^+ + e^-) \rightarrow *N_2H$ is the PDS.

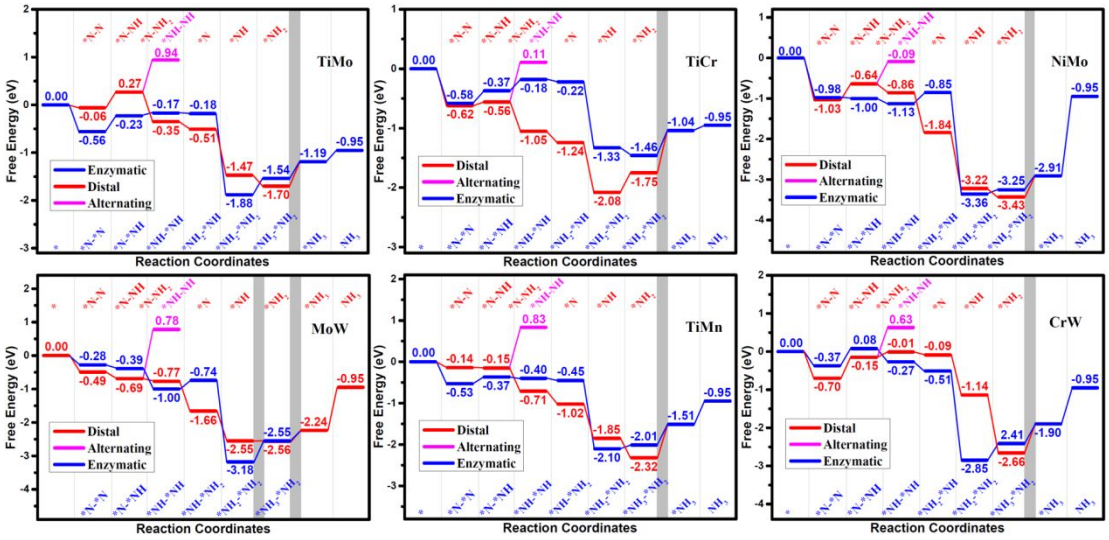

Figure S4. Free energy diagrams for NRR at zero potential on TiMo/g-C_3N_4, TiCr/g-C_3N_4, NiMo/g-C_3N_4, MoW/g-C_3N_4, TiMn/g-C_3N_4 and CrW/g-C_3N_4 along distal, alternating and enzymatic paths. The protonation process of $*NH_3NH_2/*NH_2 + (H^+ + e^-) \rightarrow *NH_3$ is the PDS.

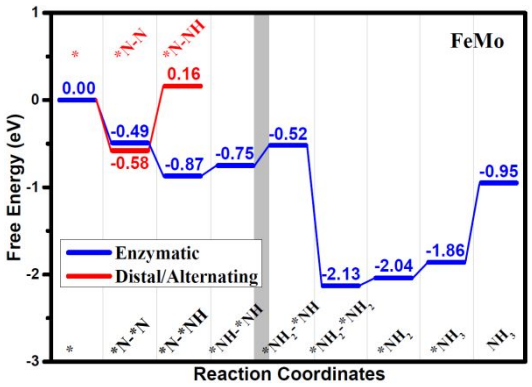

Figure S5. Free energy diagrams for NRR at zero potential on FeMo/g-C_3N_4 along distal, alternating and enzymatic mechanisms. The protonation process of *NHNH + (H^+ + e^-)→*NH_2NH is the PDS.

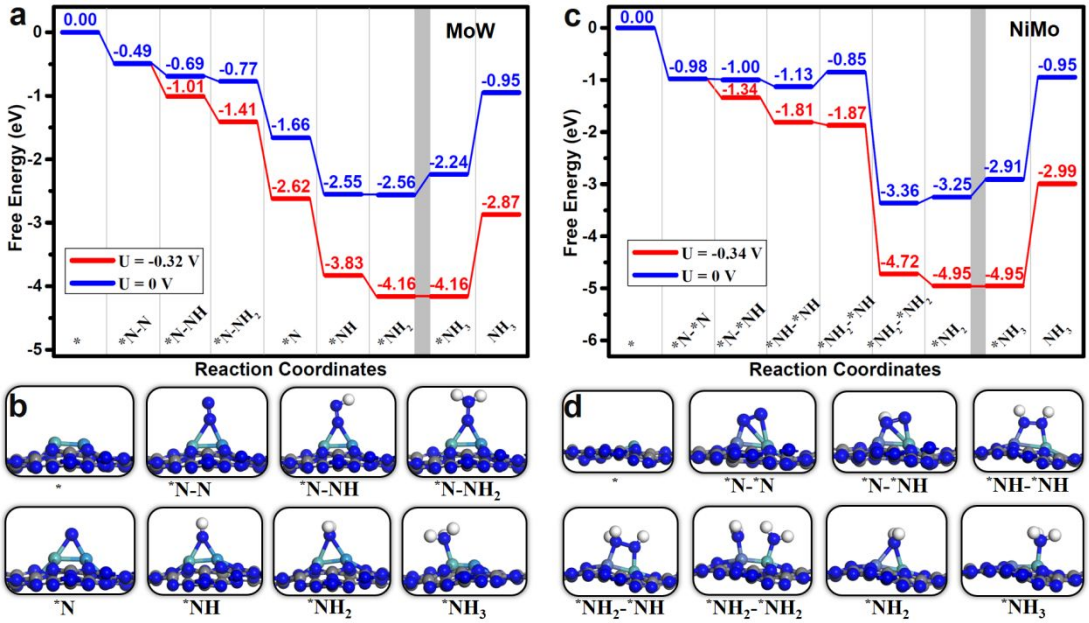

Figure S6. Free energy diagrams for the reduction of N_2 to NH_3 on **(a)** MoW/g-C_3N_4 and **(c)** NiMo/g-C_3N_4 at different applied potentials, and the corresponding configurations of NRR intermediates on **(b)** MoW/g-C_3N_4 and **(d)** NiMo/g-C_3N_4. The gray, blue, white, violet, light blue and cyan balls represent C, N, H, Ni, W and Mo atoms, respectively.

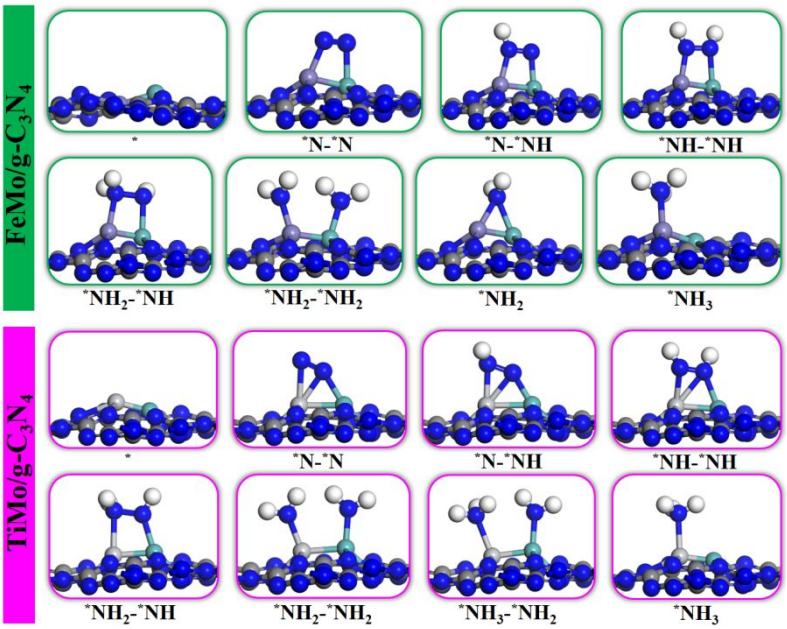

Figure S7. Optimized geometric of various intermediates along the most favorable path of NRR proceeded on FeMo/g-C_3N_4 and TiMo/g-C_3N_4. The gray, blue, white, light grey, cyan and lavender balls represent C, N, H, Ti, Mo and Fe atoms, respectively.

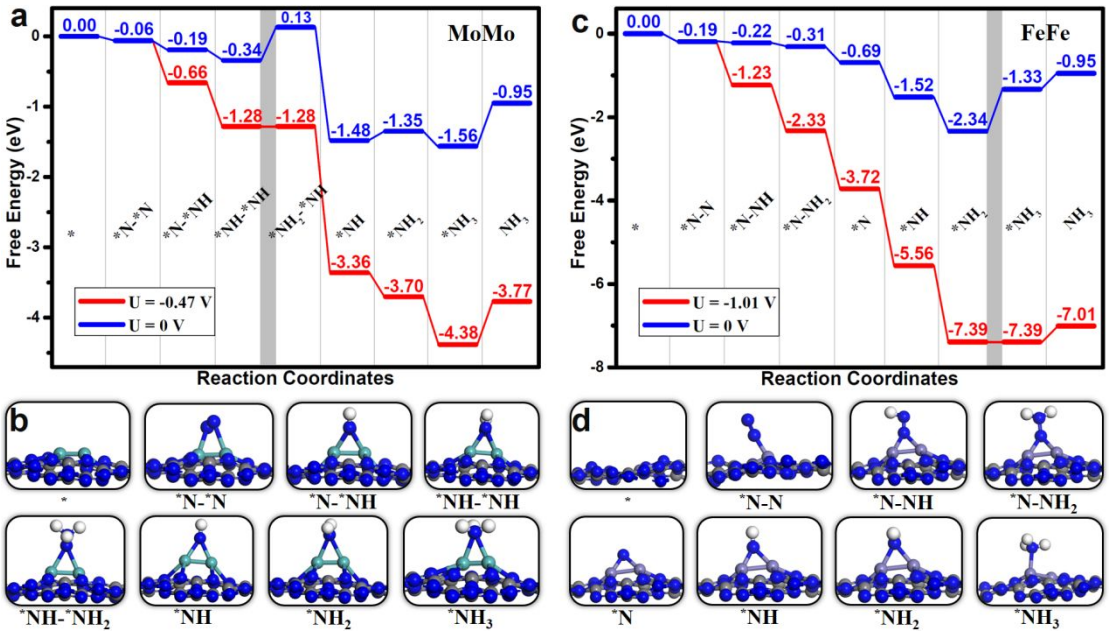

Figure S8. Free energy diagrams for the reduction of N_2 to NH_3 on **(a)** MoMo/g-C_3N_4 and **(c)** FeFe/g-C_3N_4 at different applied potentials, and the corresponding configurations of NRR intermediates on **(b)** MoMo/g-C_3N_4 and **(d)** FeFe/g-C_3N_4. The gray, blue, white, cyan and lavender balls represent C, N, H, Mo and Fe atoms, respectively.

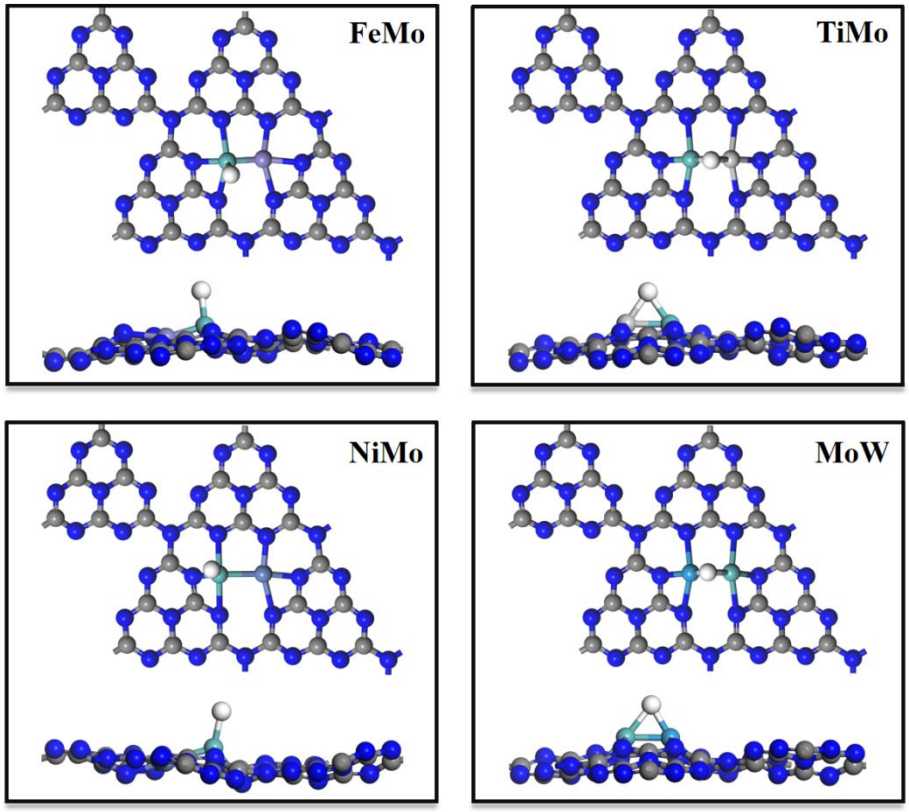

Figure S9. Optimized geometries of H* adsorbed on FeMo/g-C_3N_4, TiMo/g-C_3N_4, NiMo/g-C_3N_4 and MoW/g-C_3N_4. The gray, blue, white, light grey, cyan, lavender and violet balls represent C, N, H, Ti, Mo, Fe and Ni atoms, respectively.

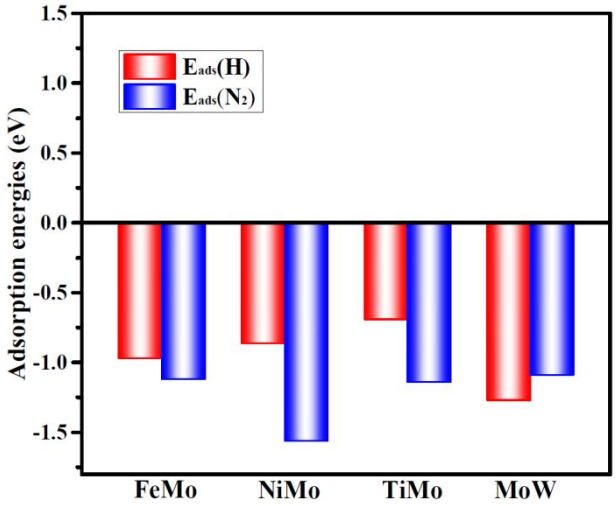

Figure S10. Comparison of the adsorption energies for *H and *N_2 on FeMo, TiMo, MoW and NiMo dual-metal catalysts.

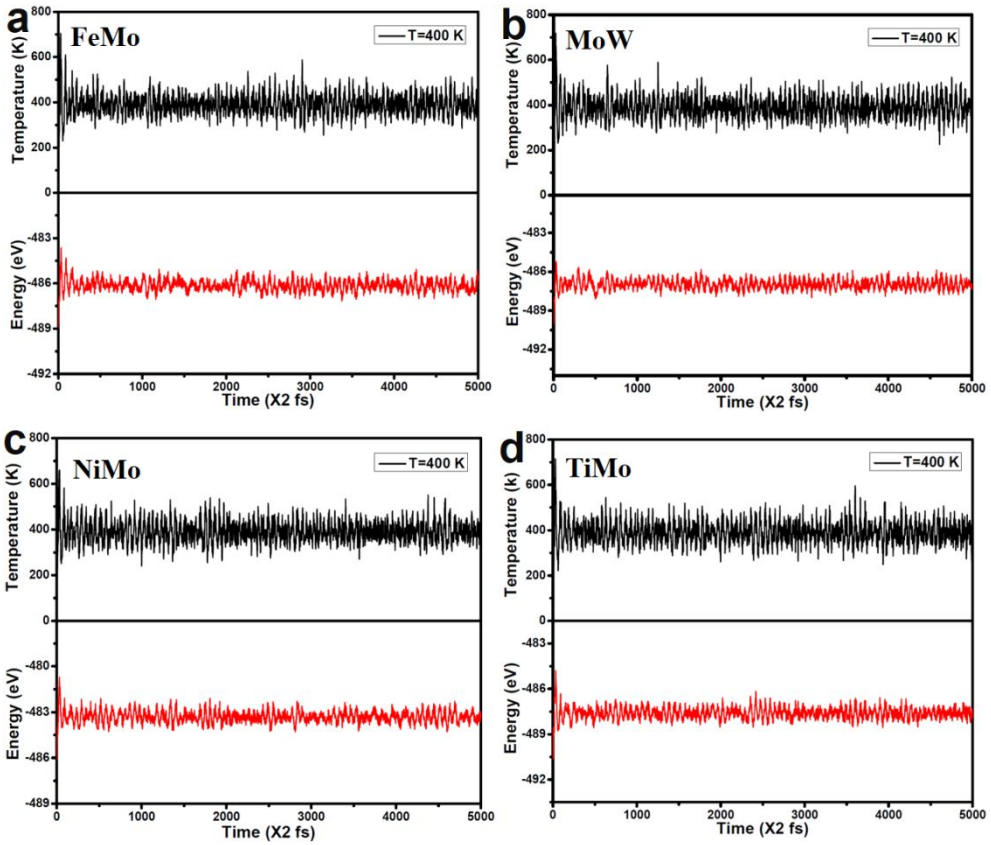

Figure S11. Variations of temperature and energy fluctuations versus the AIMD simulation time for **(a)** FeMo/g-C_3N_4, **(b)** MoW/g-C_3N_4, **(c)** NiMo/g-C_3N_4 and **(d)** TiMo/g-C_3N_4. The simulation is run under 400 K for 10 ps with a time step of 2 fs.

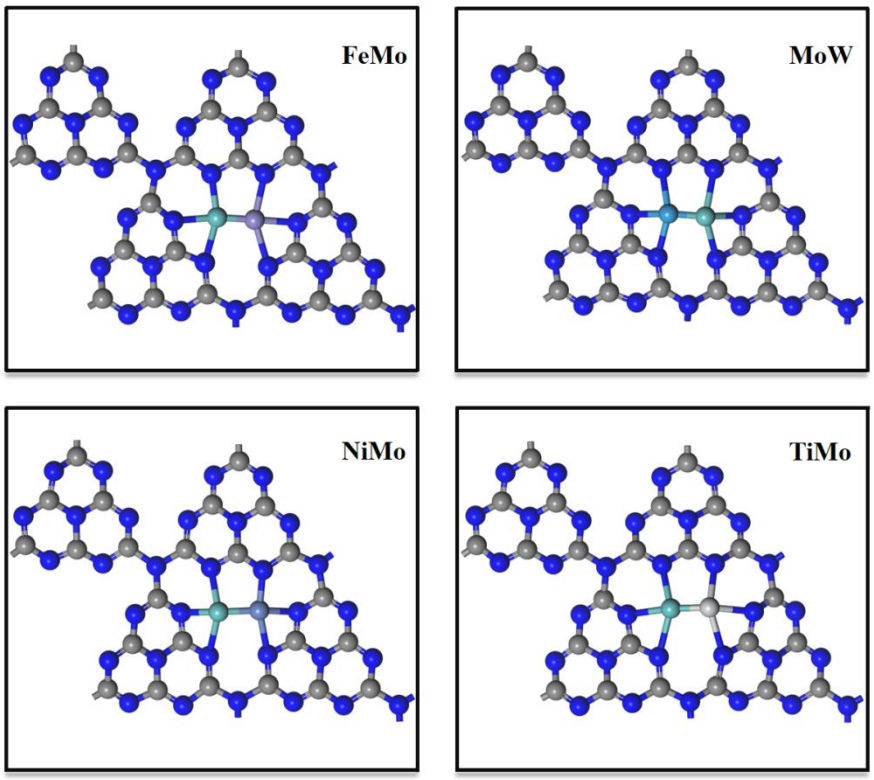

Figure S12. The snapshot of geometric structure of the last AIMD simulations step of FeMo/g-C_3N_4, MoW/g-C_3N_4, NiMo/g-C_3N_4 and TiMo/g-C_3N_4. The gray, blue, white, light grey, cyan, lavender and violet balls represent C, N, H, Ti, Mo, Fe and Ni atoms, respectively.

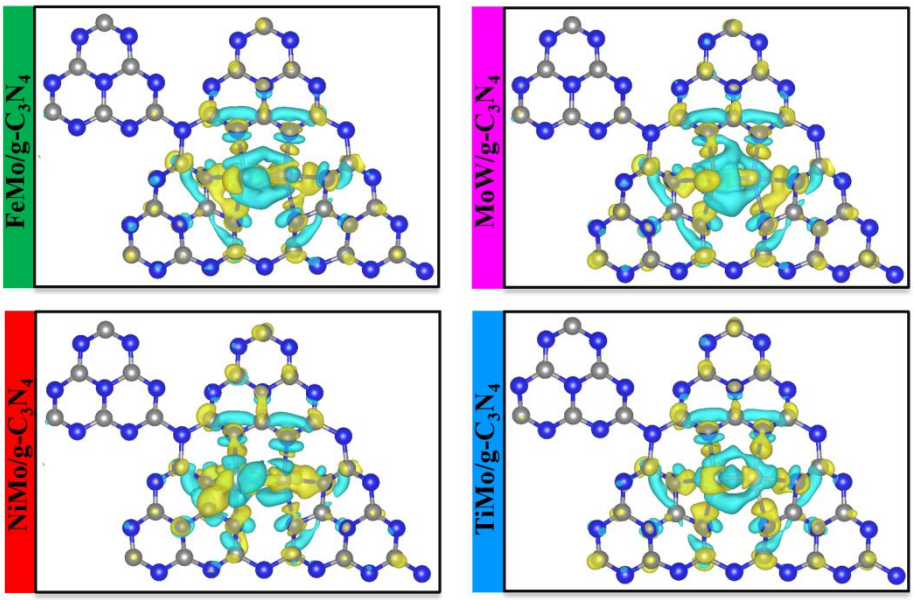

Figure S13. Charge density difference of FeMo/g-C_3N_4, MoW/g-C_3N_4, NiMo/g-C_3N_4 and TiMo/g-C_3N_4 at isosurfaces of ±0.001 e/Å^3, where the positive and negative charges are shown in yellow and cyan, respectively.

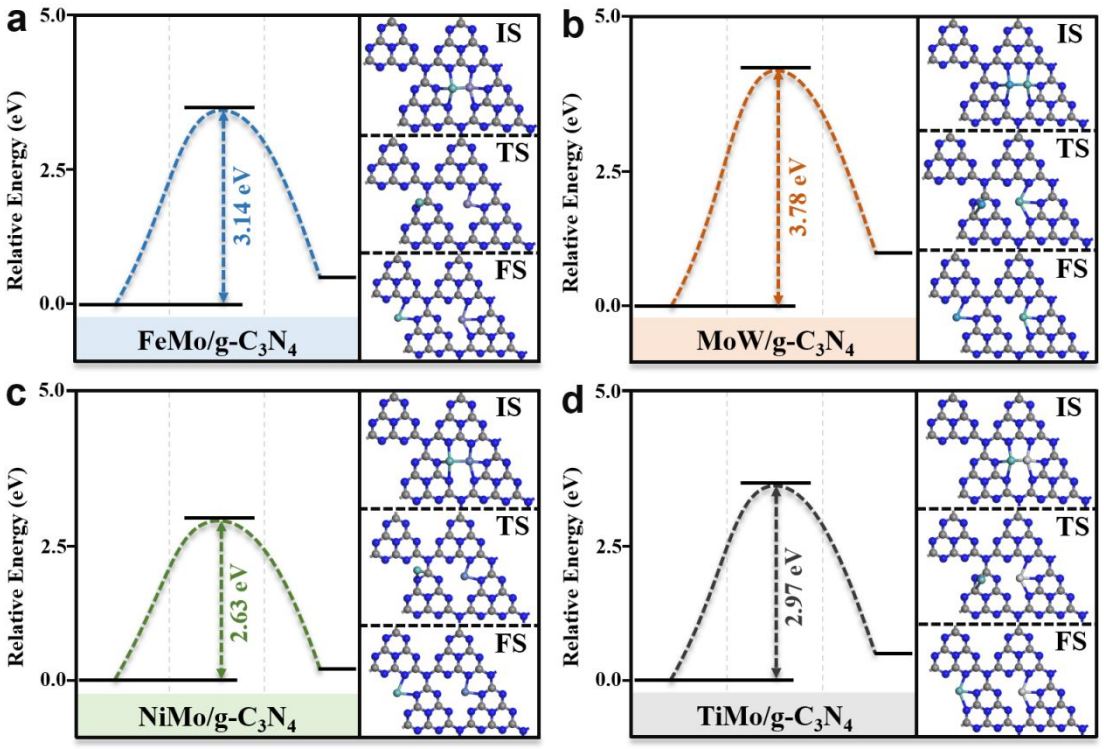

Figure S14. Atomic configurations for the dissociation of **(a)** FeMo **(b)** MoW **(c)** NiMo **(d)** TiMo dual-metals to form two separated monomers, including IS, TS, and FS. The gray, blue, white, light grey, cyan, lavender and violet balls represent C, N, H, Ti, Mo, Fe and Ni atoms, respectively.

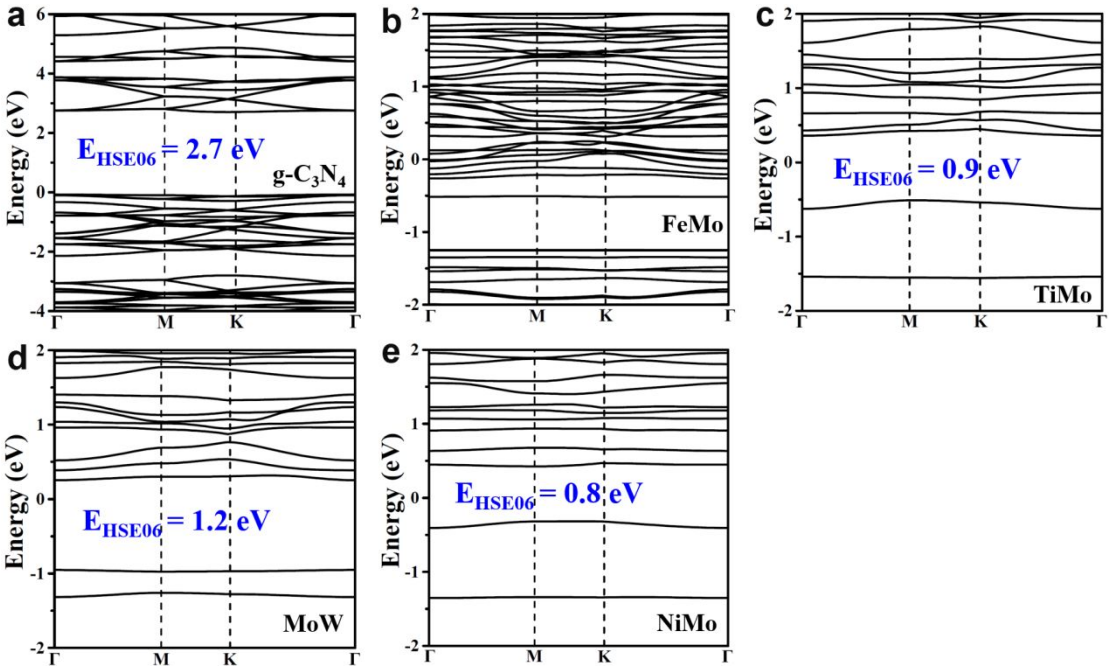

Figure S15. Electronic band structures of **(a)** pristine g-C_3N_4, **(b)** FeMo/g-C_3N_4, **(c)** TiMo/g-C_3N_4, **(d)** MoW/g-C_3N_4 and **(e)** NiMo/g-C_3N_4. The Fermi level was set to zero.

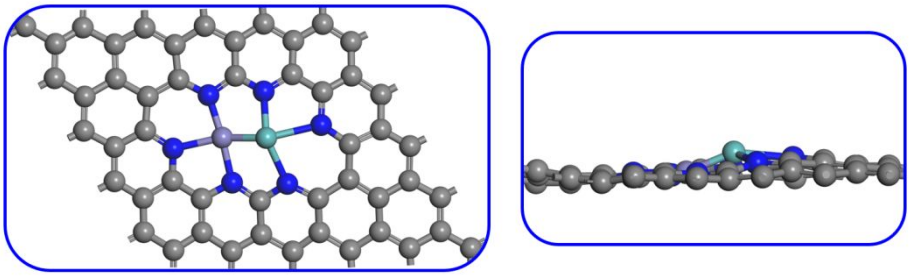

Figure S16. Top and side views of the atomic configuration of the last AIMD simulations step of FeMo/graphene. The gray, blue, cyan and lavender balls represent C, N, Mo and Fe atoms, respectively.

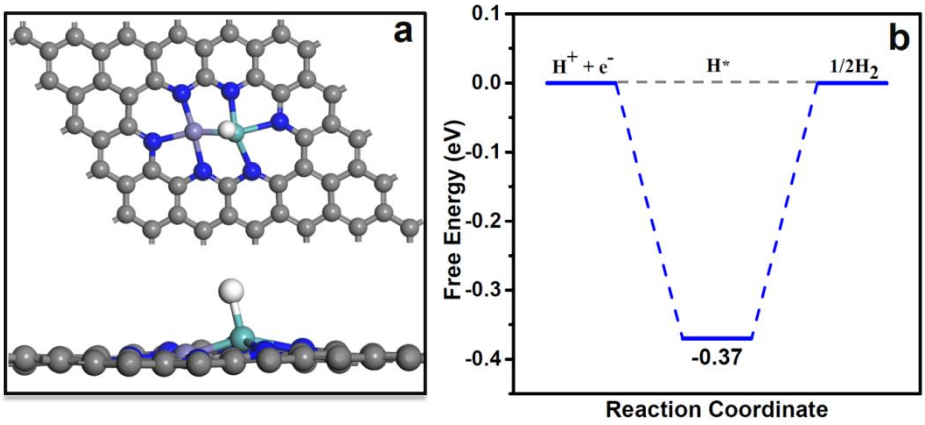

Figure S17. **(a)** Optimized geometries of H* adsorbed on FeMo/graphene. **(b)** Free energy diagrams of HER on FeMo/graphene. The gray, blue, white, cyan and lavender balls represent C, N, H, Mo and Fe atoms, respectively.

Computational details

The average binding energy of the dopant is calculated for the as following:

$$E_{\mathrm{b}} = \frac{1}{2}(E_{\mathrm{M1M2/g\text{-}C3N4}} - E_{\mathrm{g\text{-}C3N4}} - E_{\mathrm{M1}} - E_{\mathrm{M2}})$$

where $E_{\mathrm{M1M2/g\text{-}C3N4}}$, $E_{\mathrm{g\text{-}C3N4}}$, $E_{\mathrm{M1/2}}$ are the energies of M1M2/g-C3N4, substrate without metal dimer, and single metal atoms in a vacuum, respectively.

The cohesive energy of transition metal atom is calculated by the following equations:

$$E_{\mathrm{coh}} = \frac{1}{N}E_{\mathrm{TM(bulk)}} - E_{\mathrm{TM}}$$

where $E_{\mathrm{TM(bulk)}}$ is the total energy of transition metal bulk, N is the number of metal atoms in the bulk, and the E_{TM} is the energy of the relevant single metal atom in a vacuum.

The stability of the doped system is calculated as:

$$\Delta E = E_b - E_{coh}$$

To evaluate the electrochemical stabilities of the heteronuclear DACs, we systematically investigated the dissolution potential (*U*diss, versus SHE), which are defined as:

$$U_{diss} = U^o_{diss}(\text{metal, bulk}) - E_f/eN_e$$

where U^o_{diss}(metal, bulk) and N_e are the standard dissolution potential of bulk metal and the number of electrons involved in the dissolution, respectively. E_f is the formation energy of the heteronuclear metal dimers embedded in g-C_3N_4 monolayer.

The binding energy, $E_b(N)$, $E_b(N_2)$ $E_b(N_2H)$ and $E_b(NH_2)$, is defined as:

$$E_b(N) = E(N^*) - E^* - \frac{1}{2}E[N_{2(g)}]$$

$$E_b(N_2) = E(N_2^*) - E^* - E[N_{2(g)}]$$

$$E_b(N_2H) = E(N_2H^*) - E^* - E[N_{2(g)})] - \frac{1}{2}E[H_{2(g)}]$$

$$E_b(NH_2) = E(NH_2^*) - E^* - \frac{1}{2}E[N_{2(g)})] - E[H_{2(g)}]$$

where E^*, $E[_{(g)}]$ and $E(^*)$ represent the total energies of the clean slab, the isolated adsorbed molecule and the slab after adsorption, respectively.

The Gibbs free energy change (ΔG) of each elementary reaction was calculated as

$$\Delta G = \Delta E + \Delta E_{ZPE} - T\Delta S + \Delta G_{pH} + \Delta G_U + \int C_P dT$$

where ΔE is the total energy difference directly obtained from DFT calculations, ΔE_{ZPE} is the change in zero-point energies, T is the temperature, ΔS is the entropy change and C_P is the heat capacity. $\Delta G_U = -neU$, where n is the number of ($H^+ + e^-$) pairs transferred in NRR and U is the electrode potential versus the reversible hydrogen electrode (RHE). ΔG_{pH} is the correction of the H^+ free energy by the concentration, $\Delta G_{pH} = k_B T \times \ln 10 \times pH$, where k_B is the Boltzmann constant, and the value of pH was set to be zero for acidic condition. Zero-point energies and entropies of the NRR intermediates were computed from the vibrational frequencies.

The entropies of the gaseous molecules were taken from the NIST Chemistry WebBook and the zero-point energy (ZPE) was calculated according to:

$$E_{ZPE} = \sum_{i=1}^{3^N} \frac{hv_i}{2}$$

The entropy change for adsorbed intermediates was calculated within harmonic approximation:

$$\Delta S_{ads}(0\rightarrow T,P^0) = S_{vib} = \sum_{i=1}^{3N}\left[\frac{N_A h\nu_i}{T(e^{h\nu_i/K_BT}-1)} - R\ln\left(1-e^{-h\nu_i/K_BT}\right)\right]$$

Where ν_i is DFT-calculated normal-mode frequency for species of *3N* degree of freedom (*N*=number of atoms) adsorbed on M1M2/g-C_3N_4 DACs, N_A is the Avogadro's constant (6.022×10^{23} mol^{-1}), h is the Planck's constant (6.626×10^{-34}J s), and k_B is the Boltzmann constant (1.38×10^{-23} JK^{-1}), R is the ideal gas constant (8.314 J K^{-1} mol^{-1}), and T is the system temperature, and T=298K in this work. As shown in **Table S3**, ΔZPE and ΔS are the differences between the adsorbed species and the gas phase molecules in zero-point energy and entropy, respectively.

The optical absorption coefficient α(ω) was calculated from the following relation:

$$\alpha(\omega) = \sqrt{2}\frac{\omega}{c}\left[\sqrt{\varepsilon_1{}^2(\omega)+\varepsilon_2{}^2(\omega)} - \varepsilon_1(\omega)\right]^{1/2}$$

where $\varepsilon_1(\omega)$ and $\varepsilon_2(\omega)$ are the real part and imaginary part of dielectric function, respectively. The imaginary part of dielectric function is selected as the optical absorption.